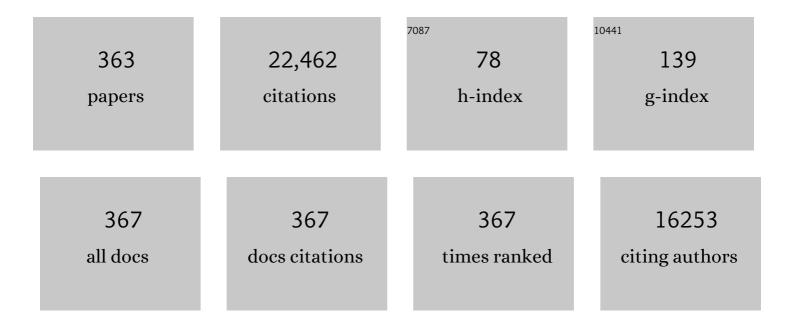
## David A Jaffray

List of Publications by Year in descending order

Source: https://exaly.com/author-pdf/1138760/publications.pdf Version: 2024-02-01



#	Article	IF	CITATIONS
1	Flat-panel cone-beam computed tomography for image-guided radiation therapy. International Journal of Radiation Oncology Biology Physics, 2002, 53, 1337-1349.	0.4	1,170
2	The use of active breathing control (ABC) to reduce margin for breathing motion. International Journal of Radiation Oncology Biology Physics, 1999, 44, 911-919.	0.4	853
3	Expanding global access to radiotherapy. Lancet Oncology, The, 2015, 16, 1153-1186.	5.1	709
4	Gold nanoparticles for applications in cancer radiotherapy: Mechanisms and recent advancements. Advanced Drug Delivery Reviews, 2017, 109, 84-101.	6.6	621
5	Gold Nanoparticles as Radiation Sensitizers in Cancer Therapy. Radiation Research, 2010, 173, 719.	0.7	547
6	Cone-beam computed tomography with a flat-panel imager: Magnitude and effects of x-ray scatter. Medical Physics, 2001, 28, 220-231.	1.6	512
7	Image-guided radiotherapy: from current concept to future perspectives. Nature Reviews Clinical Oncology, 2012, 9, 688-699.	12.5	379
8	Advances in Image-Guided Radiation Therapy. Journal of Clinical Oncology, 2007, 25, 938-946.	0.8	369
9	Prostate gland motion assessed with cine-magnetic resonance imaging (cine-MRI). International Journal of Radiation Oncology Biology Physics, 2005, 62, 406-417.	0.4	321
10	Cone-Beam Computed Tomography for On-Line Image Guidance of Lung Stereotactic Radiotherapy: Localization, Verification, and Intrafraction Tumor Position. International Journal of Radiation Oncology Biology Physics, 2007, 68, 243-252.	0.4	317
11	A radiographic and tomographic imaging system integrated into a medical linear accelerator for localization of bone and soft-tissue targets. International Journal of Radiation Oncology Biology Physics, 1999, 45, 773-789.	0.4	284
12	Accelerated partial breast irradiation using 3D conformal radiation therapy (3D-CRT). International Journal of Radiation Oncology Biology Physics, 2003, 55, 302-311.	0.4	277
13	Volume CT with a flat-panel detector on a mobile, isocentric C-arm: Pre-clinical investigation in guidance of minimally invasive surgery. Medical Physics, 2005, 32, 241-254.	1.6	275
14	Patient dose from kilovoltage cone beam computed tomography imaging in radiation therapy. Medical Physics, 2006, 33, 1573-1582.	1.6	275
15	Comparison of localization performance with implanted fiducial markers and cone-beam computed tomography for on-line image-guided radiotherapy of the prostate. International Journal of Radiation Oncology Biology Physics, 2007, 67, 942-953.	0.4	264
16	The effects of intra-fraction organ motion on the delivery of dynamic intensity modulation. Physics in Medicine and Biology, 1998, 43, 91-104.	1.6	249
17	A simple, direct method for x-ray scatter estimation and correction in digital radiography and cone-beam CT. Medical Physics, 2005, 33, 187-197.	1.6	246
18	Spektr: A computational tool for x-ray spectral analysis and imaging system optimization. Medical Physics. 2004, 31, 3057-3067.	1.6	244

#	Article	IF	CITATIONS
19	Clinical use of electronic portal imaging: Report of AAPM Radiation Therapy Committee Task Group 58. Medical Physics, 2001, 28, 712-737.	1.6	241
20	Accurate technique for complete geometric calibration of cone-beam computed tomography systems. Medical Physics, 2005, 32, 968-983.	1.6	241
21	Vulnerabilities of radiomic signature development: The need for safeguards. Radiotherapy and Oncology, 2019, 130, 2-9.	0.3	233
22	Cone-beam-CT guided radiation therapy: technical implementation. Radiotherapy and Oncology, 2005, 75, 279-286.	0.3	217
23	Irradiation of gold nanoparticles by xâ€rays: Monte Carlo simulation of dose enhancements and the spatial properties of the secondary electrons production. Medical Physics, 2011, 38, 624-631.	1.6	215
24	SlicerRT: Radiation therapy research toolkit for 3D Slicer. Medical Physics, 2012, 39, 6332-6338.	1.6	194
25	The influence of antiscatter grids on soft-tissue detectability in cone-beam computed tomography with flat-panel detectors. Medical Physics, 2004, 31, 3506-3520.	1.6	192
26	Phase 2 study of preoperative imageâ€guided intensityâ€modulated radiation therapy to reduce wound and combined modality morbidities in lower extremity soft tissue sarcoma. Cancer, 2013, 119, 1878-1884.	2.0	187
27	Intraoperative cone-beam CT for guidance of head and neck surgery: Assessment of dose and image quality using a C-arm prototype. Medical Physics, 2006, 33, 3767-3780.	1.6	186
28	The use of high-dose-rate brachytherapy alone after lumpectomy in patients with early-stage breast cancer treated with breast-conserving therapy. International Journal of Radiation Oncology Biology Physics, 2001, 50, 1003-1011.	0.4	183
29	High resolution gel-dosimetry by optical-CT and MR scanning. Medical Physics, 2001, 28, 1436-1445.	1.6	183
30	Automatic prostate localization on cone-beam CT scans for high precision image-guided radiotherapy. International Journal of Radiation Oncology Biology Physics, 2005, 63, 975-984.	0.4	182
31	Optimization of x-ray imaging geometry (with specific application to flat-panel cone-beam computed) Tj ETQq1 I	0,784314 1.6	4 rgBT /Over
32	Improvement in dose escalation using the process of adaptive radiotherapy combined with three-dimensional conformal or intensity-modulated beams for prostate cancer. International Journal of Radiation Oncology Biology Physics, 2001, 50, 1226-1234.	0.4	179
33	Inter- and Intrafractional Tumor and Organ Movement in Patients With Cervical Cancer Undergoing Radiotherapy: A Cinematic-MRI Point-of-Interest Study. International Journal of Radiation Oncology Biology Physics, 2008, 70, 1507-1515.	0.4	175
34	Online image-guided intensity-modulated radiotherapy for prostate cancer: How much improvement can we expect? A theoretical assessment of clinical benefits and potential dose escalation by improving precision and accuracy of radiation delivery. International Journal of Radiation Oncology Biology Physics, 2004, 60, 1602-1610.	0.4	161
35	A magnetic resonance imaging study of prostate deformation relative to implanted gold fiducial markers. International Journal of Radiation Oncology Biology Physics, 2007, 67, 48-56.	0.4	160
36	Costs, affordability, and feasibility of an essential package of cancer control interventions in low-income and middle-income countries: key messages from Disease Control Priorities, 3rd edition. Lancet, The, 2016, 387, 2133-2144.	6.3	156

#	Article	IF	CITATIONS
37	Characterization of scattered radiation in kV CBCT images using Monte Carlo simulations. Medical Physics, 2006, 33, 4320-4329.	1.6	155
38	Cellular uptake and transport of gold nanoparticles incorporated in a liposomal carrier. Nanomedicine: Nanotechnology, Biology, and Medicine, 2010, 6, 161-169.	1.7	152
39	Quantifying Interfraction and Intrafraction Tumor Motion in Lung Stereotactic Body Radiotherapy Using Respiration-Correlated Cone Beam Computed Tomography. International Journal of Radiation Oncology Biology Physics, 2009, 75, 688-695.	0.4	149
40	The influence of bowtie filtration on coneâ€beam CT image quality. Medical Physics, 2009, 36, 22-32.	1.6	148
41	Emergent Technologies for 3-Dimensional Image-Guided Radiation Delivery. Seminars in Radiation Oncology, 2005, 15, 208-216.	1.0	144
42	On-line aSi portal imaging of implanted fiducial markers for the reduction of interfraction error during conformal radiotherapy of prostate carcinoma. International Journal of Radiation Oncology Biology Physics, 2004, 60, 329-334.	0.4	141
43	Intracellular uptake, transport, and processing of nanostructures in cancer cells. Nanomedicine: Nanotechnology, Biology, and Medicine, 2009, 5, 118-127.	1.7	140
44	Accurate Accumulation of Dose for Improved Understanding of Radiation Effects in Normal Tissue. International Journal of Radiation Oncology Biology Physics, 2010, 76, S135-S139.	0.4	139
45	Feasibility of a novel deformable image registration technique to facilitate classification, targeting, and monitoring of tumor and normal tissue. International Journal of Radiation Oncology Biology Physics, 2006, 64, 1245-1254.	0.4	137
46	Optical-CT gel-dosimetry I: Basic investigations. Medical Physics, 2003, 30, 623-634.	1.6	136
47	The stability of mechanical calibration for a kV cone beam computed tomography system integrated	1.6	136
48	The transformation of radiation oncology using real-time magnetic resonance guidance: A review. European Journal of Cancer, 2019, 122, 42-52.	1.3	136
49	The use of adaptive radiation therapy to reduce setup error: a prospective clinical study. International Journal of Radiation Oncology Biology Physics, 1998, 41, 715-720.	0.4	133
50	Assessment of a Model-Based Deformable Image Registration Approach for Radiation Therapy Planning. International Journal of Radiation Oncology Biology Physics, 2007, 68, 572-580.	0.4	133
51	Image-Guided Radiotherapy: Has It Influenced Patient Outcomes?. Seminars in Radiation Oncology, 2012, 22, 50-61.	1.0	129
52	Radiotherapy for Cancer: Present and Future. Advanced Drug Delivery Reviews, 2017, 109, 1-2.	6.6	128
53	Fully automated treatment planning for head and neck radiotherapy using a voxel-based dose prediction and dose mimicking method. Physics in Medicine and Biology, 2017, 62, 5926-5944.	1.6	127
54	Radiation effects on the tumor microenvironment: Implications for nanomedicine delivery. Advanced Drug Delivery Reviews, 2017, 109, 119-130.	6.6	126

#	Article	IF	CITATIONS
55	Radiosensitization by gold nanoparticles: Will they ever make it to the clinic?. Radiotherapy and Oncology, 2017, 124, 344-356.	0.3	122
56	Novel dosimetric phantom for quality assurance of volumetric modulated arc therapy. Medical Physics, 2009, 36, 1813-1821.	1.6	113
57	Repeatability and reproducibility of MRI-based radiomic features in cervical cancer. Radiotherapy and Oncology, 2019, 135, 107-114.	0.3	112
58	Autoâ€segmentation of normal and target structures in head and neck CT images: A featureâ€driven modelâ€based approach. Medical Physics, 2011, 38, 6160-6170.	1.6	111
59	Respiration correlated cone-beam computed tomography and 4DCT for evaluating target motion in Stereotactic Lung Radiation Therapy. Acta Oncológica, 2006, 45, 915-922.	0.8	110
60	Setup error in radiotherapy: on-line correction using electronic kilovoltage and megavoltage radiographs. International Journal of Radiation Oncology Biology Physics, 2000, 47, 825-839.	0.4	109
61	Online ultrasound image guidance for radiotherapy of prostate cancer: impact of image acquisition on prostate displacement. International Journal of Radiation Oncology Biology Physics, 2004, 59, 595-601.	0.4	109
62	Review of image-guided radiation therapy. Expert Review of Anticancer Therapy, 2007, 7, 89-103.	1.1	109
63	Assessment of residual error in liver position using kV cone-beam computed tomography for liver cancer high-precision radiation therapy. International Journal of Radiation Oncology Biology Physics, 2006, 66, 610-619.	0.4	108
64	Cervical Cancer Regression Measured Using Weekly Magnetic Resonance Imaging During Fractionated Radiotherapy: Radiobiologic Modeling and Correlation With Tumor Hypoxia. International Journal of Radiation Oncology Biology Physics, 2008, 70, 126-133.	0.4	107
65	Generalized DQE analysis of radiographic and dual-energy imaging using flat-panel detectors. Medical Physics, 2005, 32, 1397-1413.	1.6	105
66	In Vivo Performance of a Liposomal Vascular Contrast Agent for CT and MR-Based Image Guidance Applications. Pharmaceutical Research, 2007, 24, 1193-1201.	1.7	103
67	Interfraction and Respiratory Organ Motion During Conformal Radiotherapy in Gastric Cancer. International Journal of Radiation Oncology Biology Physics, 2010, 77, 53-59.	0.4	99
68	Direct observation of ultrafast-electron-transfer reactions unravels high effectiveness of reductive DNA damage. Proceedings of the National Academy of Sciences of the United States of America, 2011, 108, 11778-11783.	3.3	99
69	Localization of Pulmonary Nodules Using Navigation Bronchoscope and a Near-Infrared Fluorescence Thoracoscope. Annals of Thoracic Surgery, 2015, 99, 224-230.	0.7	97
70	Impact of Immobilization on Intrafraction Motion for Spine Stereotactic Body Radiotherapy Using Cone Beam Computed Tomography. International Journal of Radiation Oncology Biology Physics, 2012, 84, 520-526.	0.4	96
71	Cone Beam Computed Tomography Guidance for Setup of Patients Receiving Accelerated Partial Breast Irradiation. International Journal of Radiation Oncology Biology Physics, 2007, 68, 547-554.	0.4	95
72	Active breathing control (ABC) for Hodgkin's disease: reduction in normal tissue irradiation with deep inspiration and implications for treatment. International Journal of Radiation Oncology Biology Physics, 2000, 48, 797-806.	0.4	90

#	Article	IF	CITATIONS
73	Compensators for dose and scatter management in coneâ€beam computed tomography. Medical Physics, 2007, 34, 2691-2703.	1.6	88
74	Low-dose-rate brachytherapy as the sole radiation modality in the management of patients with early-stage breast cancer treated with breast-conserving therapy: Preliminary results of a pilot trial. International Journal of Radiation Oncology Biology Physics, 1997, 38, 301-310.	0.4	87
75	Online planning and delivery technique for radiotherapy of spinal metastases using cone-beam CT: Image quality and system performance. International Journal of Radiation Oncology Biology Physics, 2007, 67, 1229-1237.	0.4	87
76	Effect of Immobilization and Performance Status on Intrafraction Motion for Stereotactic Lung Radiotherapy: Analysis of 133 Patients. International Journal of Radiation Oncology Biology Physics, 2011, 81, 1568-1575.	0.4	85
77	Spatial and temporal mapping of heterogeneity in liposome uptake and microvascular distribution in an orthotopic tumor xenograft model. Journal of Controlled Release, 2015, 207, 101-111.	4.8	84
78	Investigation of C-Arm Cone-Beam CT-Guided Surgery of the Frontal Recess. Laryngoscope, 2005, 115, 2138-2143.	1.1	81
79	Multimodal Contrast Agent for Combined Computed Tomography and Magnetic Resonance Imaging Applications. Investigative Radiology, 2006, 41, 339-348.	3.5	80
80	A quality assurance program for image quality of coneâ€beam CT guidance in radiation therapy. Medical Physics, 2008, 35, 1807-1815.	1.6	79
81	Fluence field optimization for noise and dose objectives in CT. Medical Physics, 2011, 38, S2-S17.	1.6	78
82	Intraoperative Cone-beam CT for Guidance of Temporal Bone Surgery. Otolaryngology - Head and Neck Surgery, 2006, 134, 801-808.	1.1	77
83	Energy dependence (75kVp to 18MV) of radiochromic films assessed using a real-time optical dosimeter. Medical Physics, 2007, 34, 458-463.	1.6	76
84	APN/CD13-targeting as a strategy to alter the tumor accumulation of liposomes. Journal of Controlled Release, 2011, 154, 298-305.	4.8	76
85	Full orientation invariance and improved feature selectivity of 3D SIFT with application to medical image analysis. , 2008, , .		75
86	Standardization of terminology in stereotactic radiosurgery: Report from the Standardization Committee of the International Leksell Gamma Knife Society. Journal of Neurosurgery, 2014, 121, 2-15.	0.9	75
87	Dose-volume analysis for quality assurance of interstitial brachytherapy for breast cancer. International Journal of Radiation Oncology Biology Physics, 1999, 45, 803-810.	0.4	74
88	Monte Carlo simulation on a gold nanoparticle irradiated by electron beams. Physics in Medicine and Biology, 2012, 57, 3323-3331.	1.6	74
89	Changes in apparent diffusion coefficient and T <sub>2</sub> relaxation during radiotherapy for prostate cancer. Journal of Magnetic Resonance Imaging, 2013, 37, 909-916.	1.9	74
90	Investigation of energy dependence of EBT and EBTâ€⊋ Gafchromic film. Medical Physics, 2010, 37, 571-576.	1.6	71

#	Article	IF	CITATIONS
91	An integral quality monitoring system for realâ€ŧime verification of intensity modulated radiation therapy. Medical Physics, 2009, 36, 5420-5428.	1.6	70
92	Heat-activated thermosensitive liposomal cisplatin (HTLC) results in effective growth delay of cervical carcinoma in mice. Journal of Controlled Release, 2014, 178, 69-78.	4.8	69
93	A Facility for Magnetic Resonance–Guided Radiation Therapy. Seminars in Radiation Oncology, 2014, 24, 193-195.	1.0	69
94	A Mathematical Model of the Enhanced Permeability and Retention Effect for Liposome Transport in Solid Tumors. PLoS ONE, 2013, 8, e81157.	1.1	66
95	Characterization and real-time optical measurements of the ionizing radiation dose response for a new radiochromic medium. Medical Physics, 2005, 32, 2510-2516.	1.6	65
96	Automated Weekly Replanning for Intensity-Modulated Radiotherapy of Cervix Cancer. International Journal of Radiation Oncology Biology Physics, 2010, 78, 350-358.	0.4	65
97	The intra-tumoral relationship between microcirculation, interstitial fluid pressure and liposome accumulation. Journal of Controlled Release, 2015, 211, 163-170.	4.8	65
98	Quality Assurance for the Geometric Accuracy of Cone-Beam CT Guidance in Radiation Therapy. International Journal of Radiation Oncology Biology Physics, 2008, 71, S57-S61.	0.4	64
99	Artificial intelligenceâ€based clinical decision support in modern medical physics: Selection, acceptance, commissioning, and quality assurance. Medical Physics, 2020, 47, e228-e235.	1.6	64
100	Implementation of 3D-virtual brachytherapy in the management of breast cancer: A description of a new method of interstitial brachytherapy. International Journal of Radiation Oncology Biology Physics, 1998, 40, 629-635.	0.4	63
101	Quantitative CT Imaging of the Spatial and Temporal Distribution of Liposomes in a Rabbit Tumor Model. Molecular Pharmaceutics, 2009, 6, 571-580.	2.3	62
102	Proximal Cerebral Arteries Develop Myogenic Responsiveness in Heart Failure via Tumor Necrosis Factor-α–Dependent Activation of Sphingosine-1-Phosphate Signaling. Circulation, 2012, 126, 196-206.	1.6	62
103	Hypoxia and Cellular Localization Influence the Radiosensitizing Effect of Gold Nanoparticles (AuNPs) in Breast Cancer Cells. Radiation Research, 2014, 182, 475-488.	0.7	62
104	Nanomedicine and tumor heterogeneity: Concept and complex reality. Nano Today, 2016, 11, 402-414.	6.2	59
105	Temperature and hydration effects on absorbance spectra and radiation sensitivity of a radiochromic medium. Medical Physics, 2008, 35, 4545-4555.	1.6	58
106	Technology for Innovation in Radiation Oncology. International Journal of Radiation Oncology Biology Physics, 2015, 93, 485-492.	0.4	58
107	Automatic localization of the prostate for on-line or off-line image-guided radiotherapy. International Journal of Radiation Oncology Biology Physics, 2004, 60, 623-635.	0.4	56
108	Performance of a Novel Repositioning Head Frame for Gamma Knife Perfexion and Image-Guided Linac-Based Intracranial Stereotactic Radiotherapy. International Journal of Radiation Oncology Biology Physics, 2010, 78, 306-313.	0.4	55

#	Article	IF	CITATIONS
109	An integrated approach to segmentation and nonrigid registration for application in image-guided pelvic radiotherapy. Medical Image Analysis, 2011, 15, 772-785.	7.0	55
110	Safety considerations for IGRT: Executive summary. Practical Radiation Oncology, 2013, 3, 167-170.	1.1	55
111	Radiation and Heat Improve the Delivery and Efficacy of Nanotherapeutics by Modulating Intratumoral Fluid Dynamics. ACS Nano, 2018, 12, 7583-7600.	7.3	55
112	Navigated Pelvic Osteotomy and Tumor Resection. Journal of Bone and Joint Surgery - Series A, 2015, 97, 40-46.	1.4	54
113	A quantum accounting and detective quantum efficiency analysis for video-based portal imaging. Medical Physics, 1997, 24, 815-826.	1.6	53
114	Pelvic Lymph Node Topography for Radiotherapy Treatment Planning From Ferumoxtran-10 Contrast-Enhanced Magnetic Resonance Imaging. International Journal of Radiation Oncology Biology Physics, 2009, 74, 844-851.	0.4	52
115	A Cinematic Magnetic Resonance Imaging Study of Milk of Magnesia Laxative and an Antiflatulent Diet to Reduce Intrafraction Prostate Motion. International Journal of Radiation Oncology Biology Physics, 2010, 77, 1072-1078.	0.4	52
116	Cyclophosphamide-Mediated Tumor Priming for Enhanced Delivery and Antitumor Activity of HER2-Targeted Liposomal Doxorubicin (MM-302). Molecular Cancer Therapeutics, 2015, 14, 2060-2071.	1.9	51
117	A gradient-loadable 64Cu-chelator for quantifying tumor deposition kinetics of nanoliposomal therapeutics by positron emission tomography. Nanomedicine: Nanotechnology, Biology, and Medicine, 2015, 11, 155-165.	1.7	51
118	Improving the dosimetric coverage of interstitial high-dose-rate breast implants. International Journal of Radiation Oncology Biology Physics, 2000, 46, 35-43.	0.4	49
119	Improving image-guided target localization through deformable registration. Acta Oncológica, 2008, 47, 1279-1285.	0.8	49
120	Predictors of Radiotherapy Induced Bone Injury (RIBI) after stereotactic lung radiotherapy. Radiation Oncology, 2012, 7, 159.	1.2	49
121	Tumor perfusion imaging predicts the intra-tumoral accumulation of liposomes. Journal of Controlled Release, 2013, 172, 351-357.	4.8	49
122	Ambient Mass Spectrometry Imaging with Picosecond Infrared Laser Ablation Electrospray Ionization (PIR-LAESI). Analytical Chemistry, 2015, 87, 12071-12079.	3.2	49
123	Curative-intent Metastasis-directed Therapies for Molecularly-defined Oligorecurrent Prostate Cancer: A Prospective Phase II Trial Testing the Oligometastasis Hypothesis. European Urology, 2021, 80, 374-382.	0.9	49
124	An empirical method for lag correction in coneâ€beam CT. Medical Physics, 2008, 35, 5187-5196.	1.6	48
125	Hybrid adaptive radiotherapy with on-line MRI in cervix cancer IMRT. Radiotherapy and Oncology, 2014, 110, 323-328.	0.3	48
126	Validation of biomechanical deformable image registration in the abdomen, thorax, and pelvis in a commercial radiotherapy treatment planning system. Medical Physics, 2017, 44, 3407-3417.	1.6	48

#	Article	IF	CITATIONS
127	A local shiftâ€variant Fourier model and experimental validation of circular coneâ€beam computed tomography artifacts. Medical Physics, 2009, 36, 500-512.	1.6	47
128	Dual-beam imaging for online verification of radiotherapy field placement. International Journal of Radiation Oncology Biology Physics, 1995, 33, 1273-1280.	0.4	46
129	Evaluation of the effect of patient dose from cone beam computed tomography on prostate IMRT using Monte Carlo simulation. Medical Physics, 2008, 35, 52-60.	1.6	45
130	Accuracy and sensitivity of finite element modelâ€based deformable registration of the prostate. Medical Physics, 2008, 35, 4019-4025.	1.6	45
131	A multimodal nano agent for image-guided cancer surgery. Biomaterials, 2015, 67, 160-168.	5.7	45
132	Scale-up of radiotherapy for cervical cancer in the era of human papillomavirus vaccination in low-income and middle-income countries: a model-based analysis of need and economic impact. Lancet Oncology, The, 2019, 20, 915-923.	5.1	45
133	Dosimetrically Triggered Adaptive Intensity Modulated Radiation Therapy for Cervical Cancer. International Journal of Radiation Oncology Biology Physics, 2014, 90, 147-154.	0.4	44
134	Significant Radiation Enhancement Effects by Gold Nanoparticles in Combination with Cisplatin in Triple Negative Breast Cancer Cells and Tumor Xenografts. Radiation Research, 2017, 187, 147-160.	0.7	44
135	Sensitivity of radiomic features to inter-observer variability and image pre-processing in Apparent Diffusion Coefficient (ADC) maps of cervix cancer patients. Radiotherapy and Oncology, 2020, 143, 88-94.	0.3	44
136	Measurement of Tumor Hypoxia in Patients with Advanced Pancreatic Cancer Based on <sup>18</sup> F-Fluoroazomyin Arabinoside Uptake. Journal of Nuclear Medicine, 2016, 57, 361-366.	2.8	42
137	The Exploitation of Low-Energy Electrons in Cancer Treatment. Radiation Research, 2017, 188, 123-143.	0.7	42
138	Stability of radiomic features of apparent diffusion coefficient (ADC) maps for locally advanced rectal cancer in response to image pre-processing. Physica Medica, 2019, 61, 44-51.	0.4	42
139	Machine learning helps identifying volume-confounding effects in radiomics. Physica Medica, 2020, 71, 24-30.	0.4	42
140	Wide-field tissue polarimetry allows efficient localized mass spectrometry imaging of biological tissues. Chemical Science, 2016, 7, 2162-2169.	3.7	41
141	Radiological tumour classification across imaging modality and histology. Nature Machine Intelligence, 2021, 3, 787-798.	8.3	41
142	The use of human factors methods to identify and mitigate safety issues in radiation therapy. Radiotherapy and Oncology, 2010, 97, 596-600.	0.3	40
143	MR-guided Prostate Biopsy for Planning of Focal Salvage after Radiation Therapy. Radiology, 2015, 274, 181-191.	3.6	40
144	Applying usability heuristics to radiotherapy systems. Radiotherapy and Oncology, 2012, 102, 142-147.	0.3	38

#	Article	IF	CITATIONS
145	Cone Beam Computed Tomography Image Guidance System for a Dedicated Intracranial Radiosurgery Treatment Unit. International Journal of Radiation Oncology Biology Physics, 2013, 85, 243-250.	0.4	38
146	In Vivo Optical Imaging of Tumor and Microvascular Response to Ionizing Radiation. PLoS ONE, 2012, 7, e42133.	1.1	38
147	How Advances in Imaging Will Affect Precision Radiation Oncology. International Journal of Radiation Oncology Biology Physics, 2018, 101, 292-298.	0.4	37
148	A Novel Minimally Invasive Technique to Create a Rabbit VX2 Lung Tumor Model for Nano-Sized Image Contrast and Interventional Studies. PLoS ONE, 2013, 8, e67355.	1.1	37
149	Global Task Force on Radiotherapy for Cancer Control. Lancet Oncology, The, 2015, 16, 1144-1146.	5.1	36
150	Suitability of radiochromic medium for real-time optical measurements of ionizing radiation dose. Medical Physics, 2005, 32, 1140-1155.	1.6	34
151	Dosimetric variation due to the photon beam energy in the smallâ€∎nimal irradiation: A Monte Carlo study. Medical Physics, 2010, 37, 5322-5329.	1.6	34
152	Autologous Transplantation of Lentivector/Acid Ceramidase–Transduced Hematopoietic Cells in Nonhuman Primates. Human Gene Therapy, 2011, 22, 679-687.	1.4	34
153	Use of three-dimensional radiation therapy planning tools and intraoperative ultrasound to evaluate high dose rate prostate brachytherapy implants. International Journal of Radiation Oncology Biology Physics, 1999, 43, 571-578.	0.4	33
154	Image-Guided Radiation Therapy: From Concept to Practice. Seminars in Radiation Oncology, 2007, 17, 243-244.	1.0	33
155	The need to expand global access to radiotherapy. Lancet Oncology, The, 2014, 15, 378-380.	5.1	32
156	Electron transfer-based combination therapy of cisplatin with tetramethyl- <i>p</i> -phenylenediamine for ovarian, cervical, and lung cancers. Proceedings of the National Academy of Sciences of the United States of America, 2012, 109, 10175-10180.	3.3	31
157	Contrast Agent Mass Spectrometry Imaging Reveals Tumor Heterogeneity. Analytical Chemistry, 2015, 87, 7683-7689.	3.2	31
158	Imaging Biomarker Dynamics in an Intracranial Murine Glioma Study of Radiation and Antiangiogenic Therapy. International Journal of Radiation Oncology Biology Physics, 2013, 85, 805-812.	0.4	30
159	The Use of Cone Beam Computed Tomography for Image Guided Gamma Knife Stereotactic Radiosurgery: Initial Clinical Evaluation. International Journal of Radiation Oncology Biology Physics, 2016, 96, 214-220.	0.4	30
160	The Use of Quantitative Imaging in Radiation Oncology: A Quantitative Imaging Network (QIN) Perspective. International Journal of Radiation Oncology Biology Physics, 2018, 102, 1219-1235.	0.4	30
161	Radiation Therapy for Cancer. , 2015, , 239-247.		30
162	Medical Physics, 2006, 33, 1398-1411.	1.6	29

#	Article	IF	CITATIONS
163	Intraoperative cone-beam CT for correction of periaxial malrotation of the femoral shaft: A surface-matching approach. Medical Physics, 2007, 34, 1380-1387.	1.6	29
164	Dynamic volume vs respiratory correlated 4DCT for motion assessment in radiation therapy simulation. Medical Physics, 2012, 39, 2669-2681.	1.6	29
165	Simultaneous Nonrigid Registration, Segmentation, and Tumor Detection in MRI Guided Cervical Cancer Radiation Therapy. IEEE Transactions on Medical Imaging, 2012, 31, 1213-1227.	5.4	29
166	<title>Flat-panel cone-beam CT: a novel imaging technology for image-guided procedures</title> . , 2001, , .		28
167	Softâ€tissue detectability in coneâ€beam CT: Evaluation by 2AFC tests in relation to physical performance metrics. Medical Physics, 2007, 34, 4459-4471.	1.6	28
168	Automated treatment planning for a dedicated multiâ€source intracranial radiosurgery treatment unit using projected gradient and grassfire algorithms. Medical Physics, 2012, 39, 3134-3141.	1.6	28
169	Characteristics and performance of a micro-MOSFET: An "imageable―dosimeter for image-guided radiotherapy. Medical Physics, 2004, 31, 609-615.	1.6	27
170	Liposome contrast agent for CTâ€based detection and localization of neoplastic and inflammatory lesions in rabbits: validation with FDGâ€PET and histology. Contrast Media and Molecular Imaging, 2010, 5, 147-154.	0.4	27
171	Feasibility study of a synchronizedâ€movingâ€grid (SMOG) system to improve image quality in coneâ€beam computed tomography (CBCT). Medical Physics, 2012, 39, 5099-5110.	1.6	27
172	Bringing Global Access to Radiation Therapy: Time for a Change in Approach. International Journal of Radiation Oncology Biology Physics, 2014, 89, 446-447.	0.4	27
173	Global impact of radiotherapy in oncology: Saving one million lives by 2035. Radiotherapy and Oncology, 2017, 125, 175-177.	0.3	27
174	<title>Flat-panel cone-beam CT on a mobile isocentric C-arm for image-guided brachytherapy</title> . , 2002, 4682, 209.		26
175	Twoâ€dimensional inverse planning and delivery with a preclinical image guided microirradiator. Medical Physics, 2013, 40, 101709.	1.6	25
176	Integration of optical imaging with a small animal irradiator. Medical Physics, 2014, 41, 102701.	1.6	25
177	Residual Seminal Vesicle Displacement in Marker-Based Image-Guided Radiotherapy for Prostate Cancer and the Impact on Margin Design. International Journal of Radiation Oncology Biology Physics, 2011, 80, 590-596.	0.4	23
178	Readout-segmented echo-planar diffusion-weighted imaging improves geometric performance for image-guided radiation therapy of pelvic tumors. Radiotherapy and Oncology, 2015, 117, 525-531.	0.3	23
179	Harmonic analysis for the characterization and correction of geometric distortion in MRI. Medical Physics, 2014, 41, 112303.	1.6	22
180	Treatment Age, Dose and Sex Determine Neuroanatomical Outcome in Irradiated Juvenile Mice. Radiation Research, 2015, 183, 541.	0.7	22

#	Article	IF	CITATIONS
181	Voxel-by-voxel correlation between radiologically radiation induced lung injury and dose after image-guided, intensity modulated radiotherapy for lung tumors. Physica Medica, 2017, 42, 150-156.	0.4	22
182	Preliminary Evaluation of a Novel Thermoplastic Mask System with Intra-fraction Motion Monitoring for Future Use with Image-Guided Gamma Knife. Cureus, 2016, 8, e531.	0.2	22
183	Setup Reproducibility for Thoracic and Upper Gastrointestinal Radiation Therapy: Influence of Immobilization Method and On-Line Cone-Beam CT Guidance. Medical Dosimetry, 2010, 35, 287-296.	0.4	20
184	A One-Step Cone-Beam CT-Enabled Planning-to-Treatment Model for Palliative Radiotherapy-From Development to Implementation. International Journal of Radiation Oncology Biology Physics, 2012, 84, 834-840.	0.4	20
185	Monte Carlo simulation on low-energy electrons from gold nanoparticle in radiotherapy. Journal of Physics: Conference Series, 2012, 341, 012012.	0.3	20
186	The Design and Fabrication of Carbon-Nanotube-Based Field Emission X-Ray Cathode With Ballast Resistor. IEEE Transactions on Electron Devices, 2013, 60, 464-470.	1.6	20
187	How long does it take? An analysis of volumetric image assessment time. Radiotherapy and Oncology, 2016, 119, 150-153.	0.3	20
188	Administration of Hypoxia-Activated Prodrug Evofosfamide after Conventional Adjuvant Therapy Enhances Therapeutic Outcome and Targets Cancer-Initiating Cells in Preclinical Models of Colorectal Cancer. Clinical Cancer Research, 2018, 24, 2116-2127.	3.2	20
189	Altered brain morphology after focal radiation reveals impact of off-target effects: implications for white matter development and neurogenesis. Neuro-Oncology, 2018, 20, 788-798.	0.6	20
190	Optimal radiographic magnification for portal imaging. Medical Physics, 1994, 21, 1435-1445.	1.6	19
191	2Dâ€3D registration for prostate radiation therapy based on a statistical model of transmission images. Medical Physics, 2009, 36, 4555-4568.	1.6	19
192	Automatic learningâ€based beam angle selection for thoracic IMRT. Medical Physics, 2015, 42, 1992-2005.	1.6	19
193	Professional implications of introducing artificial intelligence in healthcare: an evaluation using radiation medicine as a testing ground. Journal of Radiotherapy in Practice, 2019, 18, 5-9.	0.2	19
194	<i>In situ</i> tissue pathology from spatially encoded mass spectrometry classifiers visualized in real time through augmented reality. Chemical Science, 2020, 11, 8723-8735.	3.7	19
195	Three-dimensional NEQ transfer characteristics of volume CT using direct- and indirect-detection flat-panel imagers. , 2003, , .		18
196	Design and Fabrication of Carbon Nanotube Fieldâ€Emission Cathode with Coaxial Gate and Ballast Resistor. Small, 2013, 9, 3385-3389.	5.2	18
197	Quantitative Imaging in Radiation Oncology: An Emerging Science and Clinical Service. Seminars in Radiation Oncology, 2015, 25, 292-304.	1.0	18
198	Thermosensitive liposomal cisplatin in combination with local hyperthermia results in tumor growth delay and changes in tumor microenvironment in xenograft models of lung carcinoma <sup>*</sup> . Journal of Drug Targeting, 2016, 24, 865-877.	2.1	18

#	Article	IF	CITATIONS
199	A novel field emission microscopy method to study field emission characteristics of freestanding carbon nanotube arrays. Nanotechnology, 2017, 28, 155704.	1.3	18
200	Improved outcomes with dose escalation in localized prostate cancer treated with precision image-guided radiotherapy. Radiotherapy and Oncology, 2017, 123, 459-465.	0.3	18
201	Artificial intelligence strategy integrating morphologic and architectural biomarkers provides robust diagnostic accuracy for disease progression in chronic lymphocytic leukemia. Journal of Pathology, 2022, 256, 4-14.	2.1	18
202	Efficient on-line setup correction strategies using plan-intent functions. Medical Physics, 2006, 33, 1388-1397.	1.6	17
203	Assessment of organs-at-risk contouring practices in radiosurgery institutions around the world – The first initiative of the OAR Standardization Working Group. Radiotherapy and Oncology, 2016, 121, 180-186.	0.3	17
204	Cone-Beam Computed Tomography-Guided Navigation in Complex Osteotomies Improves Accuracy at All Competence Levels. Journal of Bone and Joint Surgery - Series A, 2018, 100, e67.	1.4	17
205	Evaluation of high dose volumetric CT to reduce inter-observer delineation variability and PTV margins for prostate cancer radiotherapy. Radiotherapy and Oncology, 2017, 125, 118-123.	0.3	16
206	Quantifying Reoxygenation in Pancreatic Cancer During Stereotactic Body Radiotherapy. Scientific Reports, 2020, 10, 1638.	1.6	16
207	Compensator models for fluence field modulated computed tomography. Medical Physics, 2013, 40, 121909.	1.6	16
208	Intra-irradiation changes in the signal of polymer-based dosimeter (GAFCHROMIC EBT) due to dose rate variations. Physics in Medicine and Biology, 2007, 52, N523-N529.	1.6	15
209	Semiautomatic vertebrae visualization, detection, and identification for online palliative radiotherapy	1.6	15
210	Automated Voxel-Based Analysis of Volumetric Dynamic Contrast-Enhanced CT Data Improves Measurement of Serial Changes in Tumor Vascular Biomarkers. International Journal of Radiation Oncology Biology Physics, 2015, 91, 48-57.	0.4	15
211	Verification of source and collimator configuration for Gamma Knife®Perfexionâ,,¢ using panoramic imaging. Medical Physics, 2010, 37, 1325-1331.	1.6	14
212	Neoplastic cell response to tiopronin-coated gold nanoparticles. Nanomedicine: Nanotechnology, Biology, and Medicine, 2013, 9, 264-273.	1.7	14
213	Whole-body organ-level and kidney micro-dosimetric evaluations of 64Cu-loaded HER2/ErbB2-targeted liposomal doxorubicin (64Cu-MM-302) in rodents and primates. EJNMMI Research, 2015, 5, 24.	1.1	14
214	User-controlled pipelines for feature integration and head and neck radiation therapy outcome predictions. Physica Medica, 2020, 70, 145-152.	0.4	14
215	<title>Performance of a volumetric CT scanner based upon a flat-panel imager</title> . , 1999, , .		13
216	Image-guided radiotherapy is being overvalued as a clinical tool in radiation oncology. Medical Physics, 2006, 33, 3583-3586.	1.6	13

#	Article	IF	CITATIONS
217	Automated 2D–3D registration of portal images and CT data using lineâ€segment enhancement. Medical Physics, 2008, 35, 4352-4361.	1.6	13
218	A method to analyze the cord geometrical uncertainties during head and neck radiation therapy using cone beam CT. Radiotherapy and Oncology, 2009, 90, 228-230.	0.3	13
219	Investigating User Perspective on Training and Clinical Implementation of Volumetric Imaging. Journal of Medical Imaging and Radiation Sciences, 2010, 41, 57-65.	0.2	13
220	Multileaf collimator performance monitoring and improvement using semiautomated quality control testing and statistical process control. Medical Physics, 2014, 41, 121713.	1.6	13
221	Tumor microenvironment determines response to a heat-activated thermosensitive liposome formulation of cisplatin in cervical carcinoma. Journal of Controlled Release, 2017, 262, 182-191.	4.8	13
222	Serial 4DCT/4DPET imaging to predict and monitor response for locally-advanced non-small cell lung cancer chemo-radiotherapy. Radiotherapy and Oncology, 2018, 126, 347-354.	0.3	13
223	Assessment of metabolite quantitation reproducibility in serial 3Dâ€≺sup>1Hâ€MR spectroscopic imaging of human brain using stereotactic repositioning. Magnetic Resonance in Medicine, 2007, 58, 666-673.	1.9	12
224	Clinical prostate T <sub>2</sub> quantification using magnetizationâ€prepared spiral imaging. Magnetic Resonance in Medicine, 2010, 64, 1155-1161.	1.9	12
225	A method for online verification of adapted fields using an independent dose monitor. Medical Physics, 2013, 40, 072104.	1.6	12
226	<i>In Vitro</i> and <i>In Vivo</i> Studies of a New Class of Anticancer Molecules for Targeted Radiotherapy of Cancer. Molecular Cancer Therapeutics, 2016, 15, 640-650.	1.9	12
227	Measurement of Tumor Hypoxia in Patients With Locally Advanced Cervical Cancer Using Positron Emission Tomography with 18F-Fluoroazomyin Arabinoside. International Journal of Radiation Oncology Biology Physics, 2018, 102, 1202-1209.	0.4	12
228	The imageâ€guided operating room—Utility and impact on surgeon's performance in the head and neck surgery. Head and Neck, 2019, 41, 3372-3382.	0.9	12
229	<title>Prototype amorphous silicon array based radiotherapy portal imager</title> . , 1997, , .		11
230	Spinal cord planning risk volumes for intensity-modulated radiation therapy of head-and-neck cancer. International Journal of Radiation Oncology Biology Physics, 2006, 64, 321-325.	0.4	11
231	Integral test phantom for dosimetric quality assurance of image guided and intensity modulated stereotactic radiotherapy. Medical Physics, 2007, 34, 1842-1849.	1.6	11
232	Automated treatment planning for a dedicated multiâ€source intraâ€cranial radiosurgery treatment unit accounting for overlapping structures and dose homogeneity. Medical Physics, 2013, 40, 091715.	1.6	11
233	Comparison of Computed Tomography– and Optical Image–Based Assessment of Liposome Distribution. Molecular Imaging, 2013, 12, 7290.2012.00028.	0.7	11
234	A novel method to quantify and compare anatomical shape: application in cervix cancer radiotherapy. Physics in Medicine and Biology, 2014, 59, 2687-2704.	1.6	11

#	Article	IF	CITATIONS
235	Custom-designed Laser-based Heating Apparatus for Triggered Release of Cisplatin from Thermosensitive Liposomes with Magnetic Resonance Image Guidance. Journal of Visualized Experiments, 2015, , e53055.	0.2	11
236	Minimally Invasive Electro-Magnetic Navigational Bronchoscopy-Integrated Near-Infrared-Guided Sentinel Lymph Node Mapping in the Porcine Lung. PLoS ONE, 2015, 10, e0126945.	1.1	11
237	Quantifying hypoxia in human cancers using static PET imaging. Physics in Medicine and Biology, 2016, 61, 7957-7974.	1.6	11
238	Monte Carlo simulation of radiation transport and dose deposition from locally released gold nanoparticles labeled with <sup>111</sup> In, <sup>177</sup> Lu or <sup>90</sup> Y incorporated into tissue implantable depots. Physics in Medicine and Biology, 2017, 62, 8581-8599.	1.6	11
239	External validation and transfer learning of convolutional neural networks for computed tomography dental artifact classification. Physics in Medicine and Biology, 2020, 65, 035017.	1.6	11
240	Development of an integral system test for image-guided radiotherapy. Medical Physics, 2004, 31, 3500-3505.	1.6	10
241	Validation of Supervised Automated Algorithm for Fast Quantitative Evaluation of Organ Motion on Magnetic Resonance Imaging. International Journal of Radiation Oncology Biology Physics, 2008, 71, 1253-1260.	0.4	10
242	Incorporating Heterogeneity Correction and 4DCT in Lung Stereotactic Body Radiation Therapy (SBRT): The Effect on Target Coverage, Organ-At-Risk Doses, and Dose Conformity. Medical Dosimetry, 2010, 35, 101-107.	0.4	10
243	Detection of point landmarks in 3D medical images via phase congruency model. Journal of the Brazilian Computer Society, 2011, 17, 117-132.	0.8	10
244	Accuracy of automatic couch corrections with onâ€line volumetric imaging <sup>*</sup> . Journal of Applied Clinical Medical Physics, 2009, 10, 106-116.	0.8	9
245	Displaying 3D radiation dose on endoscopic video for therapeutic assessment and surgical guidance. Physics in Medicine and Biology, 2012, 57, 6601-6614.	1.6	9
246	PolyMethyl Methacrylate Thin-Film-Based Field Emission Microscope. IEEE Nanotechnology Magazine, 2012, 11, 441-443.	1.1	9
247	3D imageâ€guided robotic needle positioning system for small animal interventions. Medical Physics, 2013, 40, 011909.	1.6	9
248	Automatic classification of dental artifact status for efficient image veracity checks: effects of image resolution and convolutional neural network depth. Physics in Medicine and Biology, 2020, 65, 015005.	1.6	9
249	A frequencyâ€based approach to locate common structure for 2Dâ€3D intensityâ€based registration of setup images in prostate radiotherapy. Medical Physics, 2007, 34, 3005-3017.	1.6	8
250	A method for patient dose reduction in dynamic contrast enhanced CT study. Medical Physics, 2011, 38, 5094-5103.	1.6	8
251	Geometric Performance and Efficiency of an Optical Tracking System for Daily Pre-treatment Positioning in Pelvic Radiotherapy Patients. Technology in Cancer Research and Treatment, 2011, 10, 163-170.	0.8	8
252	Self-heating Schottky emission from a ballasted carbon nanotube array. Carbon, 2013, 58, 87-91.	5.4	8

#	Article	IF	CITATIONS
253	Online virtual isocenter based radiation field targeting for high performance small animal microirradiation. Physics in Medicine and Biology, 2015, 60, 9031-9046.	1.6	8
254	Image Guided Radiation Therapy: Unlocking the Future Through Knowledge Translation. International Journal of Radiation Oncology Biology Physics, 2016, 96, 248-250.	0.4	8
255	Development and Implementation of an Electronic Learning Module for Volumetric Image-Guided Radiation Therapy. Journal of Medical Imaging and Radiation Sciences, 2016, 47, 43-48.	0.2	8
256	Coulomb explosion of vertically aligned carbon nanofibre induced by field electron emission. RSC Advances, 2017, 7, 40470-40479.	1.7	8
257	[ <sup>18</sup> F]DCFPyL PET-MRI/CT for unveiling a molecularly defined oligorecurrent prostate cancer state amenable for curative-intent ablative therapy: study protocol for a phase II trial. BMJ Open, 2020, 10, e035959.	0.8	8
258	In the Era of Deep Learning, Why Reconstruct an Image at All?. Journal of the American College of Radiology, 2021, 18, 170-173.	0.9	8
259	Incorporation of task in 3D imaging performance evaluation: the impact of asymmetric NPS on detectability. , 2004, , .		7
260	Validation of automatic landmark identification for atlas-based segmentation for radiation treatment planning of the head-and-neck region. Proceedings of SPIE, 2008, , .	0.8	7
261	Adapting population liver motion models for individualized online image-guided therapy. , 2008, 2008, 3945-8.		7
262	Automated beam model optimization. Medical Physics, 2010, 37, 2110-2120.	1.6	7
263	Excellence in Radiation Research for the 21st Century (EIRR21): Description of an Innovative Research Training Program. International Journal of Radiation Oncology Biology Physics, 2012, 83, e563-e570.	0.4	7
264	Intraoperative Near-Infrared Fluorescence-Guided Peripheral Lung Tumor Localization in Rabbit Models. Annals of Thoracic Surgery, 2019, 107, 248-256.	0.7	7
265	An artificial neural network to model response of a radiotherapy beam monitoring system. Medical Physics, 2020, 47, 1983-1994.	1.6	7
266	Flat-panel conebeam CT in the clinic: history and current state. Journal of Medical Imaging, 2021, 8, 052115.	0.8	7
267	Noise-Based Image Harmonization Significantly Increases Repeatability and Reproducibility of Radiomics Features in PET Images: A Phantom Study. Tomography, 2022, 8, 1113-1128.	0.8	7
268	<title>Unified iso-SNR approach to task-directed imaging in flat-panel cone-beam CT</title> . , 2002, , .		6
269	Volume-based radiotherapy targeting in soft tissue sarcoma. , 2004, 120, 17-42.		6
270	Prostate T <sub>1</sub> quantification using a magnetizationâ€prepared spiral technique. Journal of Magnetic Resonance Imaging, 2011, 33, 474-481.	1.9	6

#	Article	IF	CITATIONS
271	Multicenter Collaborative Quality Assurance Program for the Province of Ontario, Canada: First-Year Results. International Journal of Radiation Oncology Biology Physics, 2013, 86, 164-169.	0.4	6
272	Longitudinal tumor hypoxia imaging with [18F]FAZA-PET provides early prediction of nanoliposomal irinotecan (nal-IRI) treatment activity. EJNMMI Research, 2015, 5, 57.	1.1	6
273	Skeletonization for isocentre selection in Gamma Knife® Perfexionâ,,¢. Top, 2015, 23, 369-385.	1.1	6
274	Spatial Measurements of Perfusion, Interstitial Fluid Pressure and Liposomes Accumulation in Solid Tumors. Journal of Visualized Experiments, 2016, , .	0.2	6
275	Incorporation of delivery times in stereotactic radiosurgery treatment optimization. Journal of Global Optimization, 2017, 69, 103-115.	1.1	6
276	Dosimetric impact of intrafraction changes in MR-guided high-dose-rate (HDR) brachytherapy for prostate cancer. Brachytherapy, 2018, 17, 59-67.	0.2	6
277	Chronic Lymphocytic Leukemia Progression Diagnosis with Intrinsic Cellular Patterns via Unsupervised Clustering. Cancers, 2022, 14, 2398.	1.7	6
278	Volumetric cone-beam CT system based on a 41x41 cm2flat-panel imager. , 2001, , .		5
279	Improving quality assurance for assembled COMS eye plaques using a pinhole gamma camera. Medical Physics, 2008, 35, 4318-4323.	1.6	5
280	Macromolecule Extravasation—Xenograft Size Matters: A Systematic Study Using Probe-Based Confocal Laser Endomicroscopy (pCLE). Molecular Imaging and Biology, 2013, 15, 693-702.	1.3	5
281	Robotic path-finding in inverse treatment planning for stereotactic radiosurgery with continuous dose delivery. Medical Physics, 2016, 43, 4545-4557.	1.6	5
282	Feature-based MRI data fusion for cardiac arrhythmia studies. Computers in Biology and Medicine, 2016, 72, 13-21.	3.9	5
283	The correction of time and temperature effects in MR-based 3D Fricke xylenol orange dosimetry. Physics in Medicine and Biology, 2017, 62, 3221-3236.	1.6	5
284	Impact of tissue transport on PET hypoxia quantification in pancreatic tumours. EJNMMI Research, 2017, 7, 101.	1.1	5
285	2D–3D registration for cranial radiation therapy using a 3D kV CBCT and a single limited fieldâ€ofâ€view 2D kV radiograph. Medical Physics, 2018, 45, 1794-1810.	1.6	5
286	Spatiotemporal assessment of spontaneous metastasis formation using multimodal in vivo imaging in HER2+ and triple negative metastatic breast cancer xenograft models in mice. PLoS ONE, 2018, 13, e0196892.	1.1	5
287	Incorporating cross-voxel exchange into the analysis of dynamic contrast-enhanced imaging data: theory, simulations and experimental results. Physics in Medicine and Biology, 2021, 66, 205018.	1.6	5
288	A dual modality phantom for cone beam CT and ultrasound image fusion in prostate implant. Medical Physics, 2008, 35, 2062-2071.	1.6	4

#	Article	IF	CITATIONS
289	Investigation of intracranial peripheral dose arising from the treatment of large lesions with Leksell GammaKnife®Perfexion™. Medical Physics, 2009, 36, 2069-2073.	1.6	4
290	Simulation of field emission current uniformity of low-density freestanding CNT array. , 2010, , .		4
291	38, 2742-2753.	1.6	4
292	Editorial: Radiomics: The New World or Another Road to El Dorado?. Journal of the National Cancer Institute, 2017, 109, .	3.0	4
293	Quality control methods for linear accelerator radiation and mechanical axes alignment. Medical Physics, 2018, 45, 2388-2398.	1.6	4
294	Evaluating an Image-Guided Operating Room with Cone Beam CT for Skull Base Surgery. Journal of Neurological Surgery, Part B: Skull Base, 2021, 82, e306-e314.	0.4	4
295	Assessment of a liposomal CT/optical contrast agent for image-guided head and neck surgery. Nanomedicine: Nanotechnology, Biology, and Medicine, 2021, 32, 102327.	1.7	4
296	Image Guided Radiotherapy of the Prostate. Lecture Notes in Computer Science, 2001, , 1075-1080.	1.0	4
297	Probabilistic Refinement of Model-Based Segmentation: Application to Radiation Therapy Planning of the Head and Neck. Lecture Notes in Computer Science, 2010, , 403-410.	1.0	4
298	Predictive Radiation Oncology – A New NCI–DOE Scientific Space and Community. Radiation Research, 2022, 197, .	0.7	4
299	Comparison of computed tomography- and optical image-based assessment of liposome distribution. Molecular Imaging, 2013, 12, 148-60.	0.7	4
300	Longitudinal vascular imaging using a novel nano-encapsulated CT and MR contrast agent. , 2007, , .		3
301	Real-time optical fiber dosimeter probe. Proceedings of SPIE, 2011, , .	0.8	3
302	Reply to the comment on â€~Monte Carlo simulation on a gold nanoparticle irradiated by electron beams'. Physics in Medicine and Biology, 2013, 58, 2003-2005.	1.6	3
303	A surgical navigation system for non-contact diffuse optical tomography and intraoperative cone-beam CT. Proceedings of SPIE, 2014, , .	0.8	3
304	Automatic learning-based selection of beam angles in radiation therapy of lung cancer. , 2014, , .		3
305	Radiosurgery Nomenclature: A Confusion of Tongues. International Journal of Radiation Oncology Biology Physics, 2015, 92, 512-513.	0.4	3
306	Monte Carlo analysis of beam blocking grid design parameters: Scatter estimation and the importance of electron backscatter. Medical Physics, 2018, 45, 1059-1070.	1.6	3

#	Article	IF	CITATIONS
307	Feasibility study of navigated endoscopy for the placement of high dose rate brachytherapy applicators in the esophagus and lung. Medical Physics, 2020, 47, 917-926.	1.6	3
308	Long Circulation and Tumor Accumulation. , 2013, , 543-571.		3
309	Cancer Needs a Robust "Metadata Supply Chain―to Realize the Promise of Artificial Intelligence. Cancer Research, 2021, 81, 5810-5812.	0.4	3
310	Impact of PET scanner non-linearity on the estimation of hypoxic fraction in cervical cancer patients. Physica Medica, 2022, 93, 1-7.	0.4	3
311	126 A technique for dynamic intensity-modulated radiation therapy of the breast using a multi-leaf collimator. International Journal of Radiation Oncology Biology Physics, 1996, 36, 221.	0.4	2
312	Comparison of Correction Protocols for Image-Guided Radiation Therapy. Lecture Notes in Computer Science, 2003, , 264-270.	1.0	2
313	Fabrication and characterization of a real-time optical fiber dosimeter probe. Proceedings of SPIE, 2011, , .	0.8	2
314	A feature-based approach for refinement of Model-based segmentation of low contrast structures. , 2011, 2011, 7977-80.		2
315	Panoramic imaging of Gamma Knife is an essential test after source exchange. Medical Physics, 2013, 40, 097101.	1.6	2
316	Improved accuracy of quantitative parameter estimates in dynamic contrast-enhanced CT study with low temporal resolution. Medical Physics, 2015, 43, 388-400.	1.6	2
317	Noise distribution and denoising of current density images. Journal of Medical Imaging, 2015, 2, 024005.	0.8	2
318	Direct Lymph Node Vaccination of Lentivector/Prostate-Specific Antigen is Safe and Generates Tissue-Specific Responses in Rhesus Macaques. Biomedicines, 2016, 4, 6.	1.4	2
319	A mixed-integer optimization approach for homogeneous magnet design. Technology, 2018, 06, 49-58.	1.4	2
320	Impact of high dose volumetric CT on PTV margin reduction in VMAT prostate radiotherapy. Physics in Medicine and Biology, 2019, 64, 065017.	1.6	2
321	Fiber optic-based radiochromic dosimetry. Imaging in Medical Diagnosis and Therapy, 2016, , 293-314.	0.0	2
322	SUâ€FFâ€ŀâ€21: An Empirical Method for Lag Correction in Coneâ€Beam CT. Medical Physics, 2007, 34, 2342-23	42.6	2
323	Multi-Parametric MR Image Processing using Higher Dimensional Vector Algebra. , 2011, , .		2
324	4D-CT Attenuation Correction in Respiratory-Gated PET for Hypoxia Imaging: Is It Really Beneficial?. Tomography, 2020, 6, 241-249.	0.8	2

#	Article	IF	CITATIONS
325	Cost-function testing methodology for image-based registration of endoscopy to CT images in the head and neck. Physics in Medicine and Biology, 2020, 65, 205011.	1.6	2
326	Nanoengineered multimodal contrast agent for medical image guidance. , 2005, , .		1
327	A multi-organ biomechanical model to analyze prostate deformation due to large deformation of the rectum. , 2006, , .		1
328	Towards active image-guidance: tracking of a fiducial in the thorax during respiration under X-ray fluoroscopy. , 2007, , .		1
329	Improved CT and MR image registration with the introduction of a dual-modality contrast agent: performance assessment using quantitative and information theoretic methods. , 2008, , .		1
330	Quantitative CT Imaging of the Spatial and Temporal Distribution of Liposomes in a Rabbit Tumor Model. Molecular Pharmaceutics, 2009, 6, 1040-1040.	2.3	1
331	Delivery of smaller gold nanoparticles by liposomal incorporation. , 2010, , .		1
332	The Impact of Evolving Image-Guidance Processes on Initial Patient Setup for Lung Radiotherapy. Journal of Medical Imaging and Radiation Sciences, 2011, 42, 66-73.	0.2	1
333	Feature-driven model-based segmentation. Proceedings of SPIE, 2011, , .	0.8	1
334	Imaging in Radiation Therapy. Medical Radiology, 2011, , 63-83.	0.0	1
335	Selecting the appropriate splitter for a reflective optical fiber dosimeter probe. , 2012, , .		1
336	Monte Carlo dose calculation using a cell processor based PlayStation 3 system. Journal of Physics: Conference Series, 2012, 341, 012028.	0.3	1
337	Ballasted carbon nanotube array based X-ray tube. , 2012, , .		1
338	Technical Note: Enhancing the surface dose using a weak longitudinal magnetic field. Medical Physics, 2016, 43, 2927-2932.	1.6	1
339	Spatial frequency performance limitations of radiation dose optimization and beam positioning. Physics in Medicine and Biology, 2018, 63, 125006.	1.6	1
340	Research and innovation in global cancer control. The Lancet Global Health, 2018, 6, S1-S2.	2.9	1
341	Nanosystems for Multimodality In vivo Imaging. Fundamental Biomedical Technologies, 2008, , 409-430.	0.2	1
342	Optimization Methods for Large-Scale Radiotherapy Problems. Springer Optimization and Its Applications, 2013, , 1-20.	0.6	1

#	Article	IF	CITATIONS
343	MV and kV cone-beam CT on a medical linear accelerator. , 2000, , 561-563.		1
344	Interventional Strategies to Optimize the Delivery of Radiation Therapy. , 2002, , 116-124.		1
345	Radiation Oncology. , 2008, , 501-529.		1
346	Guidance for cone-beam CT design: tradeoff between view sampling rate and completeness of scanning trajectories. , 2006, , .		0
347	Optimization of ballasted carbon nanotube array for X-ray source. , 2013, , .		0
348	In Reply to Cheung. International Journal of Radiation Oncology Biology Physics, 2013, 85, 291-292.	0.4	0
349	Nanotechnology for Multimodality Imaging: Applications in Disease Detection and Treatment Guidance. Frontiers in Nanobiomedical Research, 2014, , 145-193.	0.1	0
350	Development of a Multi-Centre Clinical Trial Data Archiving and Analysis Platform for Functional Imaging. Journal of Physics: Conference Series, 2014, 489, 012089.	0.3	0
351	Developing Technologies for Small Animal Radiotherapy. Imaging in Medical Diagnosis and Therapy, 2016, , 329-351.	0.0	0
352	Vision 2020: looking back and thinking forward on The Lancet Oncology Commissions. Lancet Oncology, The, 2020, 21, 1144-1146.	5.1	0
353	Cone-beam computed tomography on a medical linear accelerator using a flat-panel imager. , 2000, , 558-560.		0
354	Interventional strategies to counter the effects of inter-fraction treatment variation. , 2000, , 511-513.		0
355	Radiation Therapy and Cancer Treatment: From the Basics to Combination Therapies that Ignite Immunity. , 2011, , 357-388.		0
356	Sci-Fri PM: Topics - 05: Experience with linac simulation software in a teaching environment. Medical Physics, 2014, 41, 25-25.	1.6	0
357	Chapter 6. The Role of Imaging in Nanomedicine Development and Clinical Translation. RSC Drug Discovery Series, 2016, , 151-181.	0.2	0
358	Development and clinical implementation of a hybrid system consisting of an MRI and medical linear accelerator. , 2017, , .		0
359	Editorial. Leksell Gamma Knife Society and radiosurgery: a legacy and a vision for the future. Journal of Neurosurgery, 2018, 129, 2-4.	0.9	0
360	Non-contact fluorescence tomography using a cone-beam CT surgical guidance system. , 2019, , .		0

#	Article	IF	CITATIONS
361	Image-guided fluorescence tomography in tissue phantom models of oral cancer. , 2020, , .		0
362	Improvements in SlicerRT, the radiation therapy research toolkit for 3D Slicer. , 2014, , .		0
363	Phantom Validation of a Conservation of Activity-Based Partial Volume Correction Method for Arterial Input Function in Dynamic PET Imaging. Tomography, 2022, 8, 842-857.	0.8	0